Guidance of Aircraft in Periodic Inspection Tasks

Troy S. Bruggemann and Jason J. Ford

Abstract— **This paper presents a guidance approach for aircraft in periodic inspection tasks. The periodic inspection task involves flying to a series of desired fixed points of inspection with specified attitude requirements so that requirements for downward looking sensors, such as cameras, are achieved. We present a solution using a precision guidance law and a bank turn dynamics model. High fidelity simulation studies illustrate the effectiveness of this approach under both ideal (nil-wind) and non-ideal (wind) conditions.**

I. Introduction

The benefits of using manned or robotic airborne platforms for inspection of infrastructure assets such as powerlines has been argued since the mid-1990's [1], [2], [3], [4], [5], [30]. Rotorcraft have traditionally been the platform of choice for sustained low-altitude flight above and near infrastructure for visual inspection or high resolution photography. However fixed-wing aircraft or UAV's can often achieve longer sustained flight at lower cost per distance inspected. This is important for areas where thousands of kilometers of powerline need to be inspected and cost per asset inspected is a key factor.

The requirement for low altitude fixed wing aircraft with downward-looking body-fixed cameras to capture the objects on the ground within their fixed and limited field-of-view is well acknowledged in the literature [6], [7], [8], [9], [10], [11], [12], [30]. In these applications, the aircraft itself must achieve a certain orientation, but only at the moment of inspection, so that a downward looking body-fixed camera attached to the aircraft is pointing towards the desired inspection point for images to be taken. Even if gimballed cameras are mounted, there still may be inspection attitude requirements that are not completely resolved by camera gimballing. Hence, control of both aircraft orientation and position relative to the infrastructure point under inspection must be considered. Certain features of the infrastructure (such as insulators near power poles) may need to be viewed at a certain angle using narrow field-of-view and high resolution cameras. We refer to this as the **point inspection problem**. With assets such as powerlines, often certain features of the assets spaced at regular intervals need to be inspected. We refer to this task as the **periodic inspection problem** and involves flight to and between a finite set of regular-spaced specific points of interest on the infrastructure to be inspected.

T.S. Bruggemann is with the Cooperative Research Centre for Spatial Information and Australian Research Centre for Aerospace Automation at Queensland University of Technology, 22-24 Boronia Rd, Eagle Farm, Brisbane, QLD, 4009 Australia t.bruggemann@qut.edu.au

J.J. Ford is with the Cooperative Research Centre for Spatial Information and Australian Research Centre for Aerospace Automation at Queensland University of Technology, Brisbane, QLD, 4001 Australia j2.ford@qut.edu.au

Over the past decade, there has been a considerable amount of work on Unmanned Aerial Vehicle (UAV) automation that is relevant to our aircraft automation application. A control solution for the UAV loitering problem is given in [13], a geometrical guidance law solution that accounts for camera angles to observe a ground target from a UAV is presented in [14], use of a UAV to provide 3D coverage of urban environments is given in [15], and a control solution using cameras for quasi-stationary flight above features of interest in bridge inspection is given in [16]. There has been numerous other investigation of automated tracking of targets with body-fixed or gimbaled cameras from UAVs or aircraft, see [17], [18], [19], [20], [21], [22], [23], [24], [25], [30]. These mentioned approaches typically involve the aircraft orbiting around the target in an ellipse, circle, or spiral manner whilst keeping the target in the camera field of view with possibly a desired look-angle [25]. To achieve the desired flight paths, typical approaches include waypoint placement design (e.g. [18]) or the use of commanded change of heading to track or result in a desired flight path about the ground feature to be kept within the sensor field of view (e.g. [21],[25]).

In contrast to this previous work, in this paper we propose a guidance approach for controlling the lateral motion of an aircraft so that it achieves a desired orientation (or "look angle") to a point to be inspected by body-fixed downward looking cameras at regular intervals. Our approach is based upon a simple bank turn dynamics model with an optimal precision guidance law. We aim for a solution to the periodic inspection problem which does not require special modifications to a standard autopilot, nor relies upon visual servoing. Our solution can be interfaced with existing commercially available autopilots that can accept roll or heading commands. Results from high fidelity simulations to study the effectiveness of the approach under both ideal and non-ideal (wind) conditions, are presented.

This paper is structured as follows: Section II introduces our assumed dynamic model and the periodic inspection problem. Section III present our proposed inspection approach. Section IV provide a simulation study of our proposed periodic inspection solution.

II. The Periodic Inspection Problem

The goal of periodic inspection is to achieve controlled aircraft flight to and above the infrastructure features under inspection so that they can be seen by body-fixed downward pointing sensors mounted to the aircraft. In this section, we

describe the dynamics involved, a control-loop architecture design, and then provide a formal definition of both the point inspection and periodic inspection problems.

A. Aircraft Dynamics

As shown in [30], if we assume the inspection aircraft is flying at constant speed, the aircraft's translational dynamics can be represented by

$$\begin{aligned} \dot{x} &= V\cos\chi\cos\gamma \\ \dot{y} &= V\sin\chi\cos\gamma \\ \dot{z} &= V\sin\gamma, \end{aligned} \tag{1}$$

where x, y, z is aircraft position in a navigation frame, V is the magnitude speed of the aircraft, and χ and γ are the course and flight path angles, respectively.

The evolution of χ, γ during a time period $[t_k, t_{k+1})$ can be described by the aircraft's maneuver dynamics

$$\begin{aligned} \dot{\chi} &= \frac{1}{mV\cos\gamma}\left[(L+T\sin\alpha)\sin\sigma\right. \\ &\quad \left.+(D-T\cos\alpha)\cos\sigma\sin\beta+Y\cos\sigma\cos\beta\right] \\ \dot{\gamma} &= \frac{1}{mV}\left[(L+T\sin\alpha)\cos\sigma(T\cos\alpha-D)\sin\sigma\sin\beta\right. \\ &\quad \left.-Y\sin\sigma\cos\beta\right]-\frac{1}{V}g\cos\gamma, \end{aligned} \tag{2}$$

where σ is bank angle (rotation about the velocity vector), α is angle of attack, β is angle of sideslip, L is the lift force, T is the thrust force, D is the drag force, Y is the side force and g is gravitational acceleration. Here, with pitch angle θ, the bank angle σ is related to roll angle ϕ through the expression $\cos\sigma\cos\gamma = \cos\alpha\cos\theta\cos\phi + \sin\alpha\sin\theta$ [26, p. 55].

B. Inspection Problem Definitions

We first describe the point inspection problem, before describing the periodic inspection problem.

1) The Point Inspection Problem: Let us consider a set of inspection points indexed by $i = 1, \ldots n$. The ith point inspection problem is the problem of inspecting a point $P^i = [x_P^i, y_P^i, z_P^i]$, from a specific look direction. Let the aircraft attitude in the navigation frame be denoted $\Theta = [\sigma, \gamma, \chi]$. For an aircraft at initial location $A_0^i = [x_0^i, y_0^i, z_0^i]$ and attitude $\Theta_0^i = [\sigma_0^i, \gamma_0^i, \chi_0^i]$ the problem is to guide the aircraft to intercept an inspection waypoint $WP^i = [x_{WP}^i, y_{WP}^i, z_{WP}^i]$ with altitude $z_{WP}^i = h_d^i + z_P^i$ where h_d^i is commanded height above the inspection point, and aircraft attitude Θ with the value $\Theta_d^i = \left[\phi_d^i, \theta_d^i, \psi_d^i\right]$ where $\phi_d^i, \theta_d^i, \psi_d^i$ are desired Euler roll, pitch and yaw inspection angles (designed to ensure that appropriate inspection occurs).

These aircraft position and attitude characteristics are desired at the inspection point, so that a body-fixed downward looking camera achieves inspection of fixed P^i with pointing error angle $\eta = 0$, and line of sight range error $\Delta R = R_{LOS} - R_{cam} = 0$. This situation is shown in Fig. 1 where R_{LOS} is the line of sight range from aircraft location A^i (at waypoint intercept WP^i) to P^i, and R_{cam} is the range in the direction of the downward-looking body-fixed camera boresight axis from aircraft location A^i (at waypoint intercept WP^i) to some point where it intersects the $x-y$ plane created by $z = z_P^i$. Alternatively, we can say that the point inspection guidance task $S(P^i, \Theta_d^i)$ is to inspect fixed point P^i from an aircraft with a specified desired attitude Θ_d^i (where P^i and Θ_d^i together fix the inspection waypoint WP^i).

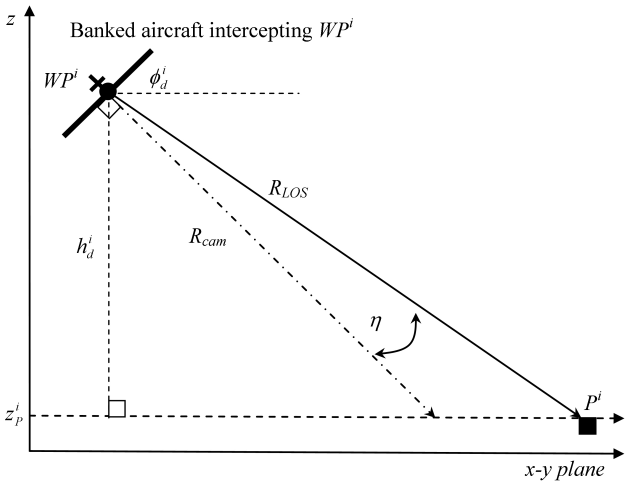

Fig. 1. Inspection geometry at inspection waypoint WP.

2) The Periodic Inspection Problem: The guidance for periodic inspection problem is now described. A periodic inspection task S_P is to achieve stable and controlled flight to inspect a set of n fixed inspection points, $\{P^i\}$, in succession; each point with an associated aircraft attitude objective, $\{\Theta_d^i\}$. That is, a periodic inspection task is defined as a control flight through the sequence of point inspection tasks described as $S_P = \{S(P^1, \Theta_d^1), S(P^2, \Theta_d^2), S(P^3, \Theta_d^3), \ldots, S(P^n, \Theta_d^n)\}$.

III. Proposed Periodic Inspection Solution

We will first propose a solution to the point inspection problem, and then will propose a solution to the periodic inspection problem.

A. Aircraft Control Loop Design

Fig. 2 shows our aircraft control loop design. The planning function determines placement of waypoints for the aircraft to commence, achieve and stop the control for inspection. The autopilot function must maintain aircraft body attitude so that infrastructure inspection can occur (this function is shown as the "dynamics with autopilot" block in the figure). We assume that the planning (waypoint design), and the autopilot block allows stable flight to meet the guidance objectives and this paper will not investigate either of these two functions.

The guidance blocks (guidance and guidance logic, in the figure) of the control loop must determine acceleration commands that minimize both the position and velocity vector mismatch between the aircraft and the inspection

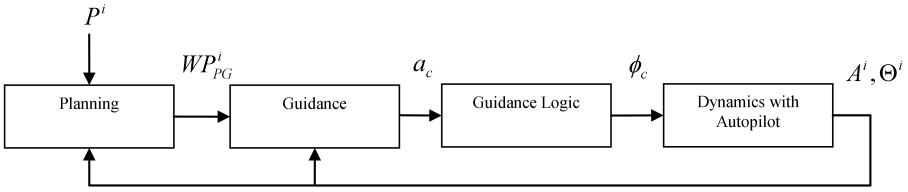

Fig. 2. The waypoint planning, guidance (and guidance logic), and autopilot functions: this paper focuses on design of the guidance and guidance logic.

point. In this paper we propose a new approach for these two blocks in following sections.

B. Altitude Control

We will assume that through-out the inspection task that constant commanded altitude is achieved at $z^i_{WP} = h^i_d + z^i_P$ by the autopilot or by a human operator. This implies that the aircraft dynamics are described by (1) with $\gamma = 0$.

C. Aircraft maneuvering restricted to bank-to-turn

The usual manner that a fixed-wing aircraft achieves a change of heading, or achieves commanded lateral acceleration, is by banking (rolling) the airframe [27]. To achieve a commanded body-fixed frame lateral acceleration a_c, the commanded roll angle ϕ_c is controlled to [6], [26], [30],

$$\phi_c = \tan^{-1}\left(\frac{a_c}{g}\right). \tag{3}$$

We will assume that u_a, u_e, and u_r are chosen so that $\beta = 0$, $Y = 0$ and also to ensure level flight in the sense that $(L + T\sin\alpha)\cos\sigma = g\cos\gamma$. Substitution in (2) shows that a BTT maneuver can be described by the dynamics [30]

$$\begin{aligned} \dot{\chi} &= \frac{g}{V}\tan\sigma \\ \dot{\phi} &= P_{roll}(\phi_c - \phi) \\ \dot{\gamma} &= 0, \end{aligned} \tag{4}$$

where P_{roll} provides a first order approximation of the autopilot's lower-level roll loop.

D. Lateral Control for Point Inspection

A lateral guidance solution that meets the Θ^i_d attitude objective is now presented. Our proposed guidance solution involves two stages, first the use of a precision guidance law to achieve control of heading to a preliminary waypoint WP^i_{PG} and secondly the activation of an open loop BTT at fixed bank angle to meet Θ^i_d attitude objectives at the desired inspection point.

This situation is shown in Fig. 3 where the aircraft flies from some starting point A^i to capture WP^i_{PG} with intercept heading angle λ^i_{WP} after which an open loop BTT is commanded over an arc distance d^i_r (θ^i_r in radians) to achieve Θ^i_d at WP^i. As shown on the figure the open loop BTT is assumed to travel the arc of a circle with turning radius r^i_d and describing the angle θ^i_{WP} between the y-axis and the radial vector at commencement of the BTT.

Our degrees of freedom are θ^i_d, ϕ^i_d, ψ^i_d and open loop BTT arc distance d^i_r. Constant altitude of flight and a small angle of attack α assumption constrains the pitch angle of inspection to be small i.e. $\theta^i_d \approx 0$. Hence, the remaining two degrees of freedom in our desired inspection attitude Θ^i_d can be described through the desired roll and yaw angles ψ^i_d and ϕ^i_d, and d^i_r is a design choice based upon prior knowledge of aircraft bank rate under autopilot control.

We propose to use an open loop BTT to achieve inspection of point $P^i = [x^i_P, y^i_P, z^i_P]$ with desired roll and heading angles ϕ^i_d and ψ^i_d. From (4) and geometry the aircraft must intercept an inspection waypoint $WP^i = [x^i_{WP}, y^i_{WP}, z^i_{WP}]$ given by

$$\begin{aligned} x^i_{WP} &= x^i_P + h^i_d \sin\psi^i_d \tan\phi^i_d \\ y^i_{WP} &= y^i_P - h^i_d \cos\psi^i_d \tan\phi^i_d \\ z^i_{WP} &= z^i_P. \end{aligned} \tag{5}$$

The desired roll angle ϕ^i_d can be achieved by commanding an open loop BTT such that $\phi_c = \phi^i_d$ for a chosen time period Δt^i_{BTT}.

This leaves the design choice ψ^i_d as the remaining degree of freedom to be controlled. Since both roll and heading angles are coupled and the aircraft cannot achieve ϕ^i_d instantaneously (but is described by (4)), the aircraft must fly for some period of flight at roll angle ϕ^i_d. This period of flight at this roll angle is a design variable which we call the lead-in arc distance of inspection (shown in Figure 3) that is denoted d^i_r or $\theta^i_r = d^i_r / r^i_d$ in radians. To allow us to appropriately design the lead-in arc distance of inspection we first note that the turn radius of the aircraft in open loop BTT [26] and the angle θ^i_{WP} are given by

$$\begin{aligned} r^i_d &= \left|\frac{V^2}{g\tan\phi^i_d}\right| \\ \theta^i_{WP} &= \frac{\pi}{2} - \psi^i_d + \theta^i_r sign(\phi^i_d). \end{aligned} \tag{6}$$

To ensure turning fixed wing aircraft flight through the desired inspection point WP^i with the desired body attitude, we need to determine an intermediate waypoint $WP^i_{PG} = [x^i_{PG}, y^i_{PG}, z^i_{PG}]$ (at some point prior to the inspection WP^i as shown in Figure 3) that places the aircraft on the BTT flight path to the inspection waypoint WP^i. The location of WP_{PG} can be calculated from geometry consideration as

$$\begin{aligned} x^i_{PG} &= x^i_P + r^i_d(\sin\theta^i_{WP} - \cos\psi^i_d) \\ y^i_{PG} &= y^i_P + r^i_d(\cos\theta^i_{WP} - \sin\psi^i_d) \\ z^i_{PG} &= z^i_P. \end{aligned} \tag{7}$$

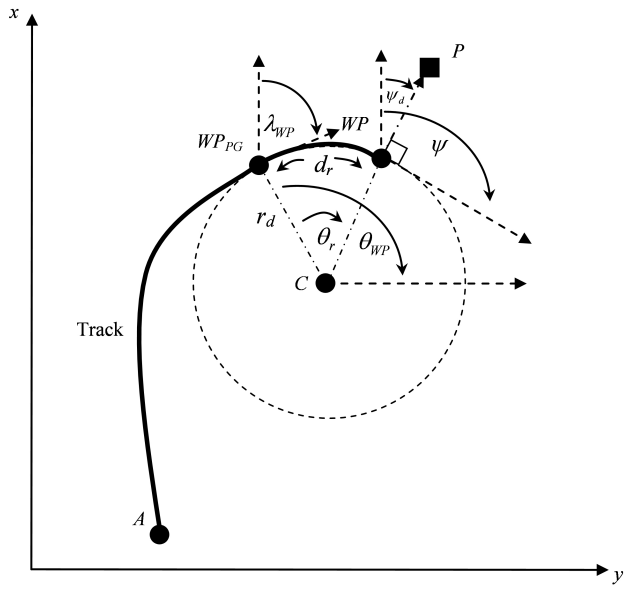

Fig. 3. Geometric representation of proposed guidance solution. Superscript "i" has been dropped from the symbols to avoid cluttering the diagram.

A required intercept heading angle λ^i_{WP} at WP^i_{PG}, defined clock-wise positive from the x-axis direction is

$$\lambda_{WP} = \frac{\pi}{2} - \theta^i_r + \psi^i_d sign(\phi^i_d). \tag{8}$$

Now that we have a solution to achieve ϕ^i_d and ψ^i_d, the final problem is to find a way to intercept WP^i_{PG} with intercept angle λ^i_{WP}. We propose to use an optimal precision guidance law which minimises the range to a waypoint and achieves desired heading at waypoint intercept [28]:

$$a_{c,PG} = V(4\dot{\lambda} + 2(\lambda - \lambda^i_{WP})/t_{go}), \tag{9}$$

where $a_{c,PG}$ is the commanded acceleration, $\lambda = \tan^{-1}(\tilde{y}/\tilde{x})$ is the line-of-sight angle with $\tilde{x} = x^i_{PG} - x$, $\tilde{y} = y^i_{PG} - y$ and $t_{go} = \sqrt{(\tilde{x})^2 + (\tilde{y})^2}/V$ is the time-to-go to WP^i_{PG}.

Finally, guidance switching logic is required to determine when to switch from the precision guidance law to the open loop BTT. The switching can be achieved when a time to go threshold t^r to WP^i_{PG} is crossed, and our complete guidance solution becomes

$$\phi_c = \begin{cases} \tan^{-1}\left(\frac{a_{c,PG}}{g}\right) & \text{when } t_{go} \geq t^r \\ \phi^i_d \text{ for } \Delta t^i_{BTT} & \text{when } t_{go} < t^r \end{cases} \tag{10}$$

E. Guidance for Periodic Inspection

Stable and controlled flight through the sequence of point inspection tasks described by $S_P = \{S(P^1, \Theta^1_d), S(P^2, \Theta^2_d), S(P^3, \Theta^3_d), \ldots, S(P^n, \Theta^n_d)\}$ is required to achieve the periodic inspection objective. The path of an aircraft is constrained due to the aircraft being an underactuated dynamical system with nonholonomic constraints. This suggests that a solution to the periodic inspection problem utilizing the guidance strategy for point inspection developed in the previous section, is in the form of a solution to a point inspection waypoint route planning problem. One solution is to order each point inspection task such that $\left\|S(P^i, \Theta^i_d) - S(P^{i+1}, \Theta^{i+1}_d)\right\| > d_{min}$, where $1 \leq i < n$ and d_{min} is a minimum distance between successive inspection points. The value of d_{min} will need to be determined by consideration of the initial starting location A_i to each point inspection task, the dynamic capabilities of the aircraft (such as maximum turn-rate) and the distance between successive inspection points.

Assuming that the point inspection waypoint route planning problem is solved, the problem is reduced to flying from one point inspection task to the next until all point inspection tasks are completed. For this purpose a third switching logic stage in the form of a PN law with $a_{c,PN} = 3V\dot{\lambda}$ is introduced into the guidance logic (10) to provide direct flight from one point inspection task to the next. Then the guidance logic for periodic inspection involves flight in PN mode until a time to go threshold t^r_{PG} to WP^i_{PG} is reached, at which point flight in PG mode and then BTT mode commences in same manner as for the point inspection task (10). This logic sequence is repeated for each ith inspection point in succession. The guidance logic repeated to each point inspection task is

$$\phi_c = \begin{cases} \tan^{-1}\left(\frac{a_{c,PN}}{g}\right) & \text{when } t_{go} \geq t^r_{PG} \\ \tan^{-1}\left(\frac{a_{c,PG}}{g}\right) & \text{when } t^r_{PG} > t_{go} \geq t^r \\ \phi^i_d \text{ for } \Delta t^i_{BTT} & \text{when } t_{go} < t^r \end{cases} \tag{11}$$

with $t^r < t^r_{PG}$.

IV. Simulation Studies

To study the performance of the proposed guidance approach, the complete control architecture shown in Fig. 1 was implemented with full six degree-of-freedom nonlinear semi-coupled equations of motion with rigid-body, fixed mass and uniform gravity assumptions for a Navion aircraft [29]. We highlight that the aircraft dynamics used in simulations had higher fidelity than those used in developing the guidance solution thus the simulation results include effects due to cross coupling between lateral and longitudinal dynamics including variations in airspeed and altitude. The autopilot loops, which included standard PID control, were tuned for aircraft stability and unchanged for all simulations. The autopilot was restricted to rate-1 (3 deg/sec) turns, to reflect roll limitations that are similar to an realistic aircraft autopilot. Airspeed of 30 m/s and inspection height h_d of 133 m was commanded. The inspection point P was set to be 5 km north of initial aircraft location $(x_0, y_0, z_0) = (0, 0, 0)$.

In this study we assume a constant lead-in arc, that is $d^i_r = d_r$ (for all i). The design choice of d_r was found to be important for good performance and must be established through experimentation. In our simulations, a d_r value of 50 m was found to give good performance in terms of roll, heading and range errors at the point. If d_r was larger, performance noticeably degraded since the aircraft flew in open loop BTT for a longer time period and this

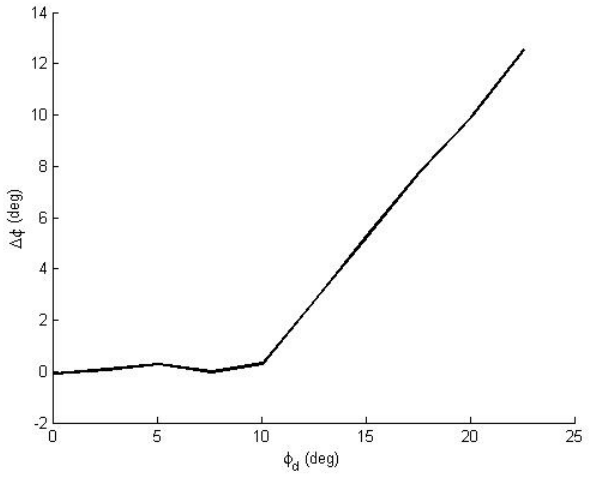

Fig. 4. Achieved roll errors for desired roll angles.

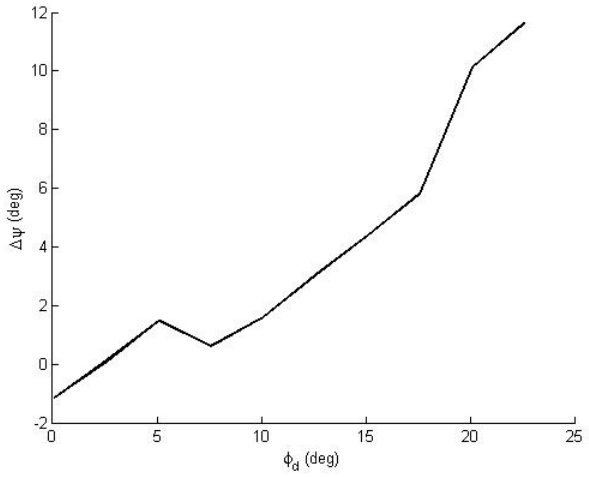

Fig. 5. Achieved heading errors for desired roll angles.

was sensitive to airspeed errors at the waypoint. If d_r was smaller however, the aircraft (depending upon aircraft bank rate under autopilot control) intercepted WP^i during the roll before the desired ϕ_d^i was achieved, causing increased roll error at the inspection point.

A. Point Inspection Studies

1) Variation of Desired Roll Angles: This study examined the performance of the proposed control solution by a simulated flight from an initial location to a fixed inspection point directly 5 km north of the initial location, in nil-wind conditions.

By keeping ψ_d^i fixed at $-10°$ the simulated flight was repeated a number of times for different $\phi_d^i = \phi_d$ values ranging from 0 to 25°. The results for all tests are summarised in Figs. 4 to 7 which plot the roll error, heading error, angular pointing error, and range error, respectively, against the respective ϕ_d. The roll and heading errors are the difference between desired and achieved values at WP^i interception. Minimum angular pointing error η and minimum range error is as defined in Fig. 1.

In Fig. 4 the roll error is near $0°$ until after $\phi_d = 10°$ where it increases due to unfulfilled roll command due to the maximum roll constraint from the autopilot rate-1 turn limitation. Similar behaviour occurs as shown in Fig. 5, 6, and 7 where it is seen that the heading angles varies to about only $2°$, minimum point error angle η less than $5°$ and minimum range error less than $1\ m$ for ϕ_d between $0°$ and $10°$. A tradeoff exists between the sensor field of view requirements and the autopilot's ability to achieve desired attitude at the inspection point. For example, assuming a minimum sensor field-of-view requirement of 2η, Fig. 6 suggests that for desired roll $0 \leq \phi_d \leq 20$ at least a $22°$ field-of-view sensor is required for the inspection point P^i to be captured.

2) Variation of Desired Heading Angles: The heading error at the inspection point is directly related to the heading error at the WP_{PG}^i which depends upon the heading error

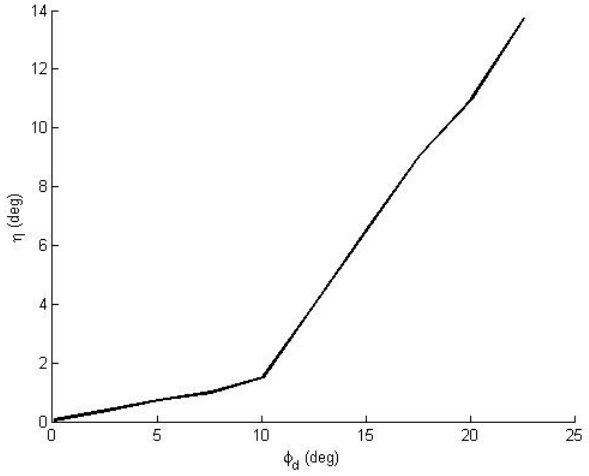

Fig. 6. Minimum angular pointing errors achieved for desired roll angles

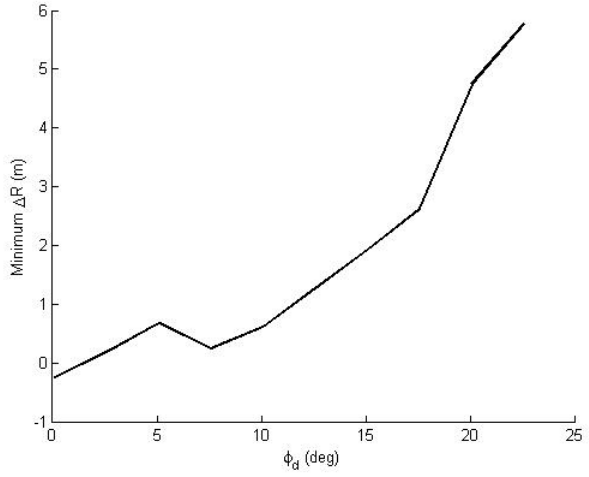

Fig. 7. Minimum range error achieved for desired roll angles

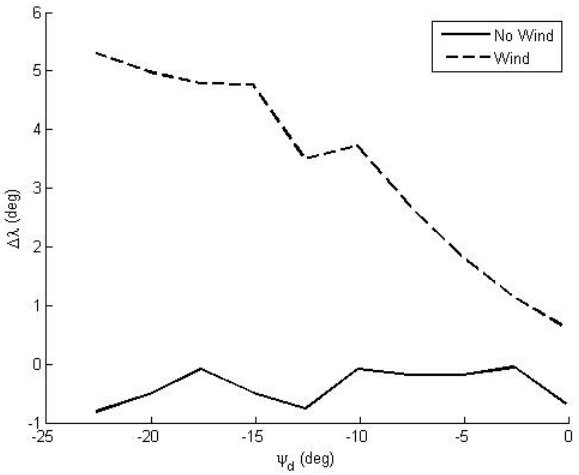

Fig. 8. PG law heading errors in nil wind and wind-present conditions.

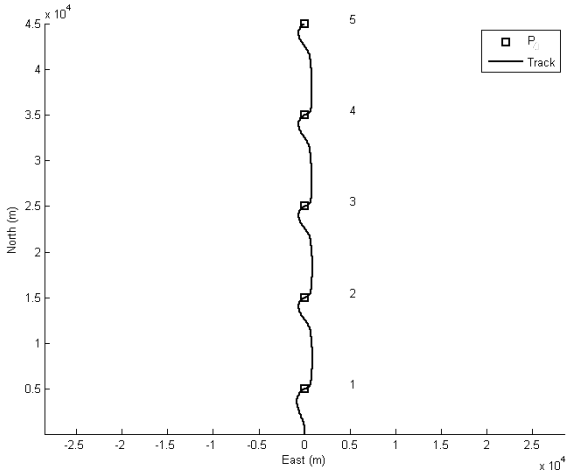

Fig. 9. Simulated flight path in periodic inspection to inspection Points 1 to 5, showing successful and stable flight to each inspection point. In the legend, Track is the ground track of the aircraft.

performance of the PG law. The aim of this test was to study the heading error performance of the PG Law in both constant wind and nil wind conditions. The test setup is the same as for the previous variation of desired heading angle study but with $\phi_d^i = \phi_d$ fixed at 10° and $\phi_d^i = \psi_d$ varied. For the constant wind case, a constant East wind of 15 knots was set throughout the simulation.

The error in achieving λ_{WP}^i for the different values of ψ_d are presented in Fig. 8. In nil wind conditions less than 1° heading error at WP_{PG}^i can be seen, however the error is increased with wind, particularly for larger ψ_d, due to the size of drift angle which depends upon the wind direction. Wind induces a heading error at WP_{PG}^i due to unaccounted drift angle in the PG law, which translates into a heading error at WP^i. If necessary, an estimate of drift angle due to wind may be included in λ_{WP}^i to mitigate unaccounted drift angle. There will also be an accumulating heading error due to wind when the aircraft is in open loop BTT mode, and this can be reduced by choosing small d_r. In these simulations, we examined the sensitivity and impact of wind on the BTT maneuver but found no improvement in performance when using a closed loop BTT technique, over an open loop BTT with short d_r, in wind-present and wind-free conditions. This suggests that there is no great benefit to be gained in adopting a more complex closed-loop BTT approach for our aircraft type under test.

B. Periodic Inspection Illustration

Here the performance of the approach in periodic inspection is illustrated by simulated flight to a set of 5 inspection points in succession in the presence of a constant East wind of 7.7 m/s, with a commanded aircraft velocity of 40 m/s and altitude of 133 m. Each point was spaced 10 km apart with desired heading angle $\psi_d^i = \psi_d = -20^\circ$ and bank angle $\phi_d^i = \phi_d = 10^\circ$ for each point.

The flight path to each inspection point 1 to 5 is shown by Fig. 9. As seen the aircraft successfully reached each inspection point objective. Flight from one point to the next

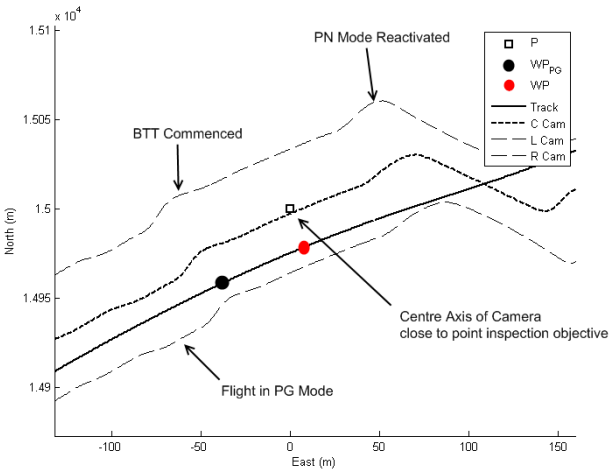

Fig. 10. Showing capture of waypoint WP_{PG} in PG mode, followed by flight in open loop BTT mode to inspection waypoint WP and achieving good alignment of the camera axis to the point inspection objective. PN Mode is then re-activated for flight to the next inspection point. In the legend, Track is the ground track of the aircraft, C Cam is the camera boresight axis, projected on the ground, L Cam is leftmost edge of the camera footprint on the ground, R Cam is rightmost edge of the camera footprint on the ground.

consists of direct flight in PN mode to a certain distance away (time to go) from a WP_{PG}^i waypoint, switching to the PG mode to capture the WP_{PG}^i waypoint with required heading angle $\bar{\lambda}$, conducting a BTT in open loop mode to achieve the look angle objectives at WP^i, followed by a re-activation of the PN mode and re-activation of the command sequences in preparation for flight to the next point. These sequences are shown in greater detail by Fig. 10, where it is seen that the sequence of commands to intercept each waypoint and the point inspection objectives are achieved.

In presence of wind and non-constant airspeed and altitude the approach was successful in achieving the ψ_d and ϕ_d

TABLE I

LINE OF SIGHT RANGE ERROR ΔR AND ANGULAR POINTING ERROR η TO EACH POINT IN PERIODIC INSPECTION.

Point	ΔR (m)	η ($^\circ$)
1	0.7	0.7
2	0.8	1.1
3	0.9	1.1
4	1.2	1.0
5	0.9	1.1

objectives with small range ΔR and angular pointing errors η as given in Table I.

V. CONCLUSIONS AND FUTURE WORKS

We presented a guidance approach for controlling an aircraft to fly to a series of desired fixed points of inspection with specified attitude requirements so that requirements for downward looking sensors such as cameras, are achieved. We presented a guidance solution using a precision guidance law and a bank turn dynamics model. High fidelity simulation studies illustrate the effectiveness of this approach under both ideal (nil-wind) and non-ideal (wind) conditions.

VI. ACKNOWLEDGMENTS

The work has been supported by the Cooperative Research Centre for Spatial Information, whose activities are funded by the Australian Commonwealth's Cooperative Research Centres Programme.

REFERENCES

[1] D.I. Jones and G.K. Earp "Requirements for aerial inspection of overhead electrical power lines", *Proc. 12th International Conf. on Remotely Piloted Vehicles*, Bristol, 1996.

[2] D.I. Jones, I. Golightly, J. Roberts, K. Usher and G.K. Earp, "Power line inspection - an UAV concept", *IEE Forum on Autonomous Systems*, London, 2006.

[3] C.C. Whitworth, A.W.G. Duller, D. Jones and G.K. Earp, "Aerial video inspection of overhead power lines", *Power Engineering Journal*, Feb, 2001.

[4] P. Campoy, P.J. Garcia, A. Barrientos, J. del Cerro, I. Aguirre, A. Roa, R. Garcia and J.M. Munoz, "An Stereoscopic Vision System Guiding an Autonomous Helicopter for Overhead Power Cable Inspection", Robot Vision, *Robot Vision, Lecture Notes in Computer Science pp. 115-124*, Springer-Verlag.

[5] Z. Li, Y. Liu, R.F. Hayward, J. Zhang, J. Cai, "Knowledge-based Power Line Detection for UAV Surveillance and Inspection Systems", *23rd International Conference on Image and Vision Computing New Zealand (IVCNZ 2008)*, Nov 26-28, Christchurch, New Zealand, USA, 2008.

[6] R.W. Beard, J.W. Curtis, M. Eilders, J. Evers and J.R. Cloutier, "Vision Aided Proportional Navigation for Micro Air Vehicles", *AIAA Guidance, Navigation and Control Conference and Exhibit*, Aug 20-23, Hilton Head, South Carolina, 2007.

[7] J. Egbert and R.W. Beard, "Low Altitude Road Following Constraints Using Strap-down EO Cameras on Miniature Aerial Vehicles", *Proceedings of the 2007 American Control Conference*, Jul 11-13, New York City, USA, 2007.

[8] E. Frew, T. McGee, Z. Kim, X. Xiao, S. Jackson, M. Morimoto, S. Rathinam, J. Padial and R. Sengupta, "Vision-Based Road-Following Using a Small Autonomous Aircraft", *IEEE Aerospace Conference*, 2004.

[9] R.S. Holt and R.W. Beard, "Vision-Based Road-Following Using Proportional Navigation", *Journal of Intelligent and Robotic Systems, 57:193-216*, 2010.

[10] S. Rathinam, Z. Kim, A. Soghikian and R. Sengupta, "Vision Based Following of Locally Linear Structures using an Unmanned Aerial Vehicle", *44th IEEE Conference on Decision and Control, and the European Control Conference*, Dec 12-15, Seville, Spain, 2005.

[11] N. Yokoyama and Y. Ochi, "Optimal Path Planning for Skid-to-Turn Unmanned Aerial Vehicle", *AIAA Guidance, Navigation and Control Conference and Exhibit*, Aug 18-21, Honolulu, Hawaii, 2008.

[12] A. Gurtner, D.G. Greer, R. Glassock, L. Mejias, R.A. Walker and W.W. Boles, "Investigation of fish-eye lenses for small-UAV aerial photography", *IEEE Transactions on Geoscience and Remote Sensing, 47(3). pp. 709-721.*, 2009.

[13] N. Regina, M. Zanzi, "2D Tracking and Over-Flight of a Target by Means of a Non-Linear Guidance Law for UAV", *Aerospace conference, 2009 IEEE* , Mar, Big Sky MT, 2009.

[14] R. Rysdyk, "Unmanned Aerial Vehicle Path Following for Target Observation in Wind", *Journal of Guidance, Control, and Dynamics*, 29: 1092-1100, 2006.

[15] P. Cheng, J. Keller and V. Kumar, "Time-Optimal UAV Trajectory Planning for 3D Urban Structure Coverage", *IEEE/RSJ International Conference on Intelligent Robots and Systems*, Sep. 22-26, 2008.

[16] N. Metni and T. Hamel, "Visual Tracking Control of Aerial Robotic Systems with Adaptive Depth Estimation", *International Journal of Control, Automation, and Systems*, 5:1, pp. 51-60, Feb. 2007.

[17] J. Saunders, R. Beard, "Tracking a Target in Wind Using a Micro Air Vehicle with a Fixed Angle Camera", *American Control Conference, 2009 IEEE* , Mar, Big Sky MT, 2009.

[18] S. M. Farrell, D. R. Jacques, "Waypoint Generation based upon Sensor Aimpoint", *EMAV 2009*

[19] D. Lee, I. Kaminer, V. Dobrokhodov, K. Jones, "Autonomous Feature Following for Visual Surveillance Using a Small Unmanned Aerial Vehicle with Gimbaled Camera System", *International Journal of Control, Automation, and Systems (2010) 8(5):957-966*

[20] N. Ceccarelli, J. J. Enright, E. Frazzoli, S. J. Rasmussen, C. J. Schumacher, "Micro UAV Path Planning for Reconnaissance in Wind", *Proceedings of the 2007 American Control Conference*, New York, 2007.

[21] S. Stolle, R. Rysdyk, "Flight Path Following Guidance for Unmanned Air Vehicles with Pan-tilt Camera for Target Observation", *22nd Digital Avionics Systems Conference, 2003*.

[22] F. Le Bras, T. Hamel, R. Mahony, "Image-based Visual Servo Control for Circular Trajectories for a Fixed-Wing Aircraft", *Joined 48th IEEE Conference on Decision and Control and 28th Chinese Control Conference*, Shanghai,China, Dec 2009.

[23] P. Theodorakopoulos, S. Lacroix, "A strategy for tracking a ground target with a UAV", *2008 IEEE/RSJ International Conference on Intelligent Robots and Systems*, Nice, France, Sept 2008.

[24] N. R. Gans, J. Shen, J. W. Curtis, "Selection of a UAV Orbit to Keep Multiple Targets in the Camera Field of View", *2010 IEEE International Symposium on Intelligent Control*, Yokohama, Japan, Sept 2010.

[25] P.G. Thomasson, "Guidance of a roll-only camera for ground observation in wind", *Journal of Guidance, Control, and Dynamics, 21(1):39-48, January 1998*.

[26] R.F. Stengel, *Flight Dynamics*, Princeton University Press, Princeton, 2004.

[27] D. McLean, Automatic Flight Control Systems, Prentice Hall, New York, 1990.

[28] J. Ford, "Precision Guidance with Impact Angle Requirements", *Aeronautical and Maritime Research Laboratory, Defence Science and Technology Organisation, 2001*.

[29] M. Sadraey, R. Colgren, "UAV Flight Simulation: Credibility of Linear Decoupled vs. Nonlinear Coupled Equations of Motion", *AIAA Conference*, Aug, San Francisco, 2005.

[30] T.S. Bruggemann, J. J. Ford, R.A. Walker, "Control of Aircraft for Inspection of Linear Infrastructure." *IEEE Transactions on Control Systems Technology*,2010, url:http://dx.doi.org/10.1109/TCST.2010.2093937.